Lawrence Berkeley National Laboratory
LBL Publications

Title
'Candidatus Adiutrix intracellularis', an endosymbiont of termite gut flagellates, is the first representative of a deep-branching clade of Deltaproteobacteria and a putative homoacetogen

Permalink
https://escholarship.org/uc/item/08v1q91p

Journal
Environmental Microbiology, 18(8)

ISSN
1462-2912

Authors
Ikeda-Ohtsubo, Wakako
Strassert, Jürgen FH
Köhler, Tim
et al.

Publication Date
2016-09-01

DOI
10.1111/1462-2920.13234

Peer reviewed

'Candidatus Adiutrix intracellularis', a homoacetogenic deltaproteobacterium colonizing the cytoplasm of termite gut flagellates (Trichonympha collaris)

SCHOLARONE™
Manuscripts

'*Candidatus* Adiutrix intracellularis', a homoacetogenic deltaproteobacterium colonizing the cytoplasm of termite gut flagellates (*Trichonympha collaris*)

Wakako Ikeda-Ohtsubo[1†], Jürgen F. H. Strassert[1,2], Tim Köhler[1], Aram Mikaelyan[1], Ivan Gregor[3,4], Alice C. McHardy[3,4], Susannah Green Tringe[5], Phil Hugenholtz[5,6], Renate Radek[2], and Andreas Brune[1]*

[1] *Department of Biogeochemistry, Max Planck Institute for Terrestrial Microbiology, Karl-von-Frisch-Strasse 10, 35043 Marburg, Germany*

[2] *Institute of Biology/Zoology, Free University of Berlin, Königin-Luise-Strasse 1–3, 14195 Berlin, Germany*

[3] *Computational Biology of Infection Research, Helmholtz Center for Infection Research, Inhoffenstraße 7, 38124 Braunschweig, Germany*

[4] *Department of Algorithmic Bioinformatics, Heinrich Heine University Düsseldorf, 40225 Düsseldorf, Germany*

[5] *Department of Energy Joint Genome Institute, Walnut Creek, California 94598, USA*

[6] *Australian Centre for Ecogenomics, The University of Queensland, Brisbane QLD 4072, Australia*

Running title: *A homoacetogenic deltaproteobacterium from termite guts*

*For correspondence. E-mail brune@mpi.marburg.mpg.de; Tel. (+49) 6421 178701

[†] Present address: Laboratory of Animal Products Chemistry, Graduate School of Agricultural Science, Tohoku University, Sendai 981-8555, Japan

1 **Summary**

2 Termite gut flagellates are typically colonized by specific bacterial symbionts. Here we

3 describe the phylogeny, ultrastructure, and subcellular location of '*Candidatus* Adiutrix

4 intracellularis', an intracellular symbiont of *Trichonympha collaris* in the termite

5 *Zootermopsis nevadensis*. It represents a novel, deep-branching lineage of uncultured

6 *Deltaproteobacteria* widely distributed in intestinal tracts of termites and cockroaches.

7 Fluorescence in situ hybridization and transmission electron microscopy revealed that the

8 symbiont colonizes the cytoplasm of the flagellate near hydrogenosomes in the posterior part

9 of the host cell and near the ectosymbiont '*Candidatus* Desulfovibrio trichonymphae' in the

10 anterior part. The draft genome of '*Ca.* Adiutrix intracellularis' ($\sim$2 Mbp; > 91% complete)

11 obtained from a metagenomic library allowed us to assess its metabolic potential. The

12 presence of a complete gene set encoding the Wood-Ljungdahl pathway, including a

13 hydrogen-dependent carbon dioxide reductase (HDCR), substantiates previous claims that the

14 symbiont is capable of reductive acetogenesis from CO_2 and H_2. The HDCR genes are most

15 closely related to homologs from homoacetogenic spirochetes and firmicutes, suggesting that

16 the deltaproteobacterium acquired the capacity for homoacetogenesis via lateral gene transfer.

17 The presence of genes for an alternative nitrogenase (AnfHDK) and the biosynthesis of

18 essential amino acids and co-factors indicate the nutritional nature of the symbiosis.

19

20

21

22 Keywords: *termite gut flagellates, intracellular symbionts, reductive acetogenesis, hydrogen,*

23 *Deltaproteobacteria*

24

Introduction

26 Flagellate protists are abundant and characteristic members of the gut microbiota in lower

27 termites (Brune and Ohkuma, 2011; Brune 2014). Originally described as "parasites" (Leidy,

28 1881), their essential role in the symbiotic digestion of lignocellulose was established already

29 during the first half of the 20th century (Cleveland, 1925; Hungate 1943). Flagellates of the

30 genus *Trichonympha* (class Parabasalia) are found in members of several termite families, and

31 their diversity has been described in numerous morphological and molecular studies (see

32 Kirby, 1932; Brugerolle and Radek, 2006; Carpenter et al., 2009; Ohkuma et al., 2009).

33 Most termite gut flagellates are colonized by specific bacterial symbionts, often in multiple

34 associations (Hongoh and Ohkuma, 2011; Ohkuma and Brune, 2011). Some of them represent

35 deep-branching lineages that were most likely acquired by ancestral flagellates at an early

36 stage of their evolutionary radiation. In the genus *Trichonympha*, examples are '*Candidatus*

37 Endomicrobium trichonymphae' (Stingl et al., 2005), which belongs to a termite-specific

38 clade in the Elusimicrobia phylum and occurs exclusively in flagellates of *Trichonympha*

39 Cluster I (Ohkuma et al., 2007; Ikeda-Ohtsubo and Brune, 2009), and '*Candidatus* Ancillula

40 trichonymphae', a lineage in a termite-specific clade of *Actinobacteria* that occurs in

41 flagellates of *Trichonympha* cluster II (Strassert et al., 2012).

42 While such "primary" symbionts seem to have cospeciated with their respective hosts over a

43 longer evolutionary time frame (Noda et al., 2007; Ikeda-Ohtsubo and Brune, 2009; Desai et

44 al., 2010), there are many examples of "secondary" symbionts that were independently

45 acquired by individual host species, most likely long after the symbiosis with the primary

46 symbiont had been established (Ohkuma and Brune, 2011). A prominent example of such

47 recent associations is '*Candidatus* Desulfovibrio trichonymphae', which colonizes either the

48 cytoplasm (in *Reticulitermes speratus*) or cell surface (in *Incisitermes marginipennis*) of

49 *Trichonympha* species (Sato et al., 2009; Strassert et al., 2012) and belongs to a lineage within

50 the *Desulfovibrio* complex that is commonly encountered also in the intestinal tracts of

51 flagellate-free termites and other insects.

52 However, diversity studies of termite gut microbiota have identified also a second, much more

53 deep-branching clade of *Deltaproteobacteria*, the 'Rs-K70 group' (e.g., Hongoh et al., 2003;

54 2005; Shinzato et al, 2007; Warnecke et al., 2007), which was abundantly represented in clone

55 libraries of bacterial 16S rRNA genes obtained from capillary-picked *Trichonympha*

56 suspensions of the dampwood termite *Zootermopsis nevadensis* (JQ993543; Ikeda-Ohtsubo

57 2007, Strassert et al., 2012). Rosenthal et al. (2013) localized transcripts of a hydrogenase-

58 linked formate dehydrogenase gene (fdhF$_{Sec}$) to single cells of an almost identical phylotype

59 (JX974519) of uncultured *Deltaproteobacteria* from the gut of this termite and documented

60 its association with *Trichonympha* flagellates. The observations that the homolog assigned to

61 the symbiont was the most highly expressed fdhF$_{Sec}$ gene in the gut implicated this flagellate

62 symbiont – and possibly also other members of the Rs-K70 group – as major players in

63 reductive acetogenesis from H_2 and CO_2 in termite guts (Rosenthal et al., 2013).

64 Here we provide a detailed phylogenetic, ultrastructural, and metabolic characterization of an

65 endosymbiont '*Candidatus* Adiutrix intracellularis', from this Rs-K70 group. We analyzed its

66 relationship to other members of the Rs-K70 group from the intestinal tracts of insects and

67 determined its host specificity and subcellular location by fluorescence in situ hybridization

68 (FISH) and transmission electron microscopy (TEM). In addition, we reconstructed the

69 metabolism of the endosymbiont from its draft genome, which was assembled from a

70 metagenomic library prepared from genomic DNA of the microbial symbionts associated with

71 the *Trichonympha* flagellates of *Z. nevadensis*.

Results and discussion

72

Phylogeny

73

74 The 16S rRNA gene sequences of '*Ca.* Adiutrix intracellularis' previously obtained from

75 capillary-picked *Trichonympha* suspensions consisted of several, almost identical phylotypes

76 (99.4–99.9% sequence similarity) that clustered among other representatives of the Rs-K70

77 group recovered from the intestinal tracts of termites (Fig. 1). With a specific primer pair

78 designed on the basis of these sequences, we obtained additional clones from hindgut DNA of

79 several cockroaches (*Blaberus giganteus*, *Gromphadorrhina portentosa*, and *Nauphoeta*

80 *cinerea*), lower termites (*Zootermopsis nevadensis, Cryptotermes secundus*), and a cetoniid

81 beetle larva (*Pachnoda ephippiata*). Together with several clones recently obtained from other

82 termites and cockroaches (Mikaelyan et al., 2015), they all clustered according to their

83 respective host groups (Fig. S1). Interestingly, the clones from *Z. nevadensis* comprised

84 additional, previously unknown phylotypes that were distinct from '*Ca.* Adiutrix

85 intracellularis' and may represent symbionts of other flagellate species or free-living members

86 of the Rs-K70 group.

87 The next relatives of the clones in the Rs-K70 group are uncultured bacteria from terrestrial

88 and marine environments (Fig. 1). '*Ca.* Adiutrix intracellularis' shares only very low sequence

89 similarity (86.1–86.6%) with the 16S rRNA genes of its closest cultured relatives, namely

90 *Desulfatiglans* (*Desulfobacterium*) *anilini*, *Desulfoarculus baarsii*, and *Desulfomonile tiedjei*,

91 which are each considered to represent a different order of *Deltaproteobacteria* (Kuever,

92 2014), underlining the deep-branching nature of the novel lineage.

93 ***Localization***

94 FISH analysis of *Trichonympha* suspensions from *Z. nevadensis* with a newly designed

95 oligonucleotide probe revealed that '*Ca.* Adiutrix intracellularis' exclusively colonized

96 flagellates with the morphology of *Trichonympha collaris* (Fig. 2). Host specificity was

97 confirmed by simultaneous hybridization with a probe specific for this flagellate species (Fig.

98 S2A–D). Cells of '*Ca.* Adiutrix intracellularis' were distributed throughout the cytoplasm of

99 the host cell, but showed highest densities in the anterior region, which is characterized by the

100 brighter, concentrated signal on the collar (Fig. 2A, C; Fig. S2B, D). The location of '*Ca.*

101 Adiutrix intracellularis' differs from that of '*Ca.* Endomicrobium trichonymphae', which

102 preferentially colonizes the posterior part of the cell (Ikeda-Ohtsubo and Brune, 2009; Fig.

103 S2E, F).

104 Flagellates of the genus *Trichonympha* are often colonized by '*Ca.* Desulfovibrio

105 trichonymphae', which forms a monophyletic lineage of uncultivated *Deltaproteobacteria* in

106 termite guts. Originally identified as endosymbionts of *Trichonympha agilis* in *Reticulitermes*

107 *speratus* (Sato et al., 2008), a member of this lineage has also been detected in capillary-

108 picked *Trichonympha* suspensions of *Z. nevadensis* (Strassert et al., 2012). Simultaneous

109 hybridization of *T. collaris* with FISH probes specific for '*Ca.* Adiutrix intracellularis' and

110 '*Ca.* Desulfovibrio trichonymphae' confirmed that the former are found throughout the host

111 cell, whereas the latter are restricted to the anterior part, oriented in rows parallel to the

112 surface grooves (Fig. 2D).

113   *Ultrastructure*

114   TEM of ultrathin sections of *Trichonympha* cells from *Z. nevadensis* confirmed the

115   simultaneous presence of bacterial cell types with distinct morphologies in the anterior region.

116   One morphotype consists of short, irregular rods of variable diameter (0.5–0.6 μm) and length

117   (0.8–1.9 μm; $n = 25$). The cells have slightly pointed ends and a somewhat irregular

118   appearance. The wide electron-lucent space surrounding the cytoplasmic membrane has a

119   highly contrasted outermost border, which resembles an outer membrane of the symbiont

120   more than a vacuolar membrane of the host (Fig. 3A). The cells are characterized by electron-

121   dense glycogen-like granules in their cytoplasm and were observed both in the anterior and

122   posterior part of the host cell. In the posterior region, they were often situated close to

123   hydrogenosomes (Fig. 3A). In the anterior part, they colonized the cytoplasmic protrusions

124   between the multiple rows of flagella (Fig. 3B), the rostral tube, and the anterior cell pole

125   (Fig. S3). Their morphology, subcellular arrangement and intracellular distribution were

126   consistent with those of '*Ca.* Adiutrix intracellularis' in the FISH analyses (Fig. 2, Fig. S3).

127   The other morphotype is also rod-shaped, but much smaller (0.2–0.3 μm diameter, 1.1–1.9

128   μm length; $n = 13$), with a regular circumference and rounded ends (Fig. 3B). The cells are

129   located on the surface of the cytoplasmic lamellae, often in proximity to cells of the first

130   morphotype (Fig. 3B, C), and are laterally attached in deep pockets of the cytoplasmic

131   membrane of the host. Occasionally, cells of the second morphotype were observed also

132   within the cytoplasm of *Trichonympha* flagellates (not shown). These features are consistent

133   with the morphology and distribution of '*Ca.* Desulfovibrio trichonymphae' in the FISH

134   analyses (Fig. 2D). The regular arrangement of the cells along the cytoplasmic lamellae of the

135   host cell (Fig. 3B) closely resembles the situation of the *Desulfovibrio* ectosymbionts of

136   *Trichonympha globulosa* in *Incisitermes marginipennis* (Strassert et al. 2012).

137   The results of our current study provided an opportunity to revisit the exquisite work of

138   Harold Kirby (1932), who has provided a detailed morphological description of the

139   *Trichonympha* species in *Zootermopsis* termites on the basis of light microscopy. His

140   observation of multiplying "peripheral granules" in the anterior end of *T. collaris* (collar and

141   following surface ridges; Fig. S3) and his description of the rostrum having "the appearance

142   of a collar striped with granular bands" bear a striking resemblance to the FISH micrographs

143   of the dual hybridization of '*Ca.* Adiutrix intracellularis' and '*Ca.* Desulfovibrio

144   trichonymphae' (Fig. 2D).

Genome sequence

A 16S rRNA gene library prepared from genomic DNA of the microbial symbionts associated with a suspension of *Trichonympha* flagellates from *Z. nevadensis* yielded 353 bacterial clones. The majority of the clones (50%) represented '*Endomicrobium trichonymphae*', the primary endosymbiont of these flagellates (Ikeda-Ohtsubo, 2007; Strassert et al., 2012). The second largest group (21%) was '*Ca.* Adiutrix intracellularis', followed by '*Ca.* Desulfovibrio trichonymphae' (17%) and other, much less abundant groups (for details, see Table S1). The majority of the 73 clones assigned to '*Ca.* Adiutrix intracellularis' represented the phylotype Adiu1 (AB972401), which is identical to that recovered in our previous studies (JQ993543; Ikeda-Ohtsubo 2007, Strassert et al., 2012).

The draft genome of strain Adiu1 (IMG Genome ID: 2556793040) was obtained through shotgun sequencing of this DNA, followed by sequence assembly and a combination of automated and manual binning. The sequence bin of strain Adiu1 consists of 155 scaffolds (2,076,491 bp) and has an N50 value of 23,926, which is much higher than that of any other bin in the dataset (Table S1). The draft genome contains one set of rRNA genes, 48 tRNA genes for all amino acids, and a near complete set (> 91%) of single-copy genes present in most bacterial genomes, including the most-closely related *Deltaproteobacteria* (Garcia Martin et al., 2006; Table S2).

The estimated genome size of strain Adiu1 is much smaller (ca. 2.3 Mb) and its coding density (60.1%) is much lower than the genome size and coding density in its closest relatives, *Dg. anilini* (4.67 Mb, 85.2%) and *Da. baarsii* (3.66 Mb, 91.1%), which indicated genome erosion in the endosymbiont. Also the G+C content of the genome is considerably lower in strain Adiu1 (43.3 mol%) than in its relatives (58.8 and 65.7 mol%, respectively). Almost the half (46.2%) of the 1,520 protein-coding genes in the Adiu1 genome gave highest BLAST scores against the genomes of other *Deltaproteobacteria* (Table S3). Of these genes, the majority had best matches against *Desulfobacterales* (27%), *Desulfovibrionales* (25%), and *Syntrophobacterales* (16%); the rest was either unassigned (22%) or showed an affinity to other phylogenetic groups (e.g., *Firmicutes*, 11%; *Gammaproteobacteria*, 3.5%). Such apparent heterogeneity in the phylogenetic origin of the coding genes is present also in *Da. baarsii* and *Dg. anilini*, which is not entirely unexpected considering that each of these strains represents a separate, deep-branching lineage of *Deltaproteobacteria* that is only poorly represented among sequenced genomes (Table S3; Suzuki et al., 2014).

Wood-Ljungdahl pathway

Although the closest relatives of '*Ca.* Adiutrix intracellularis' are sulfate-reducing *Deltaproteobacteria*, the draft genome of strain Adiu1 lacks the genes for key enzymes of sulfate reduction (Table S4). This includes *dsrAB* encoding alpha and beta subunits of dissimilatory sulfite reductase, *aprAB* for adenosine-5'-phosphosulfate reductase (APS reductase), *sat* for sulfate adenylyltransferase (ATP sulfurylase), and *sulP* for a sulfate permease (SulP). Also genes for cytochrome synthesis (i.e., the heme-specific branch of the tetrapyrrole biosynthesis pathway) and other important elements involved in sulfate reduction (e.g., Qmo and DsrMKJOP) were not found.

Instead, the genome contains the complete set of genes required for the Wood–Ljungdahl pathway of reductive acetogenesis (Table S4 and S5; Schuchmann and Müller, 2014). They include homologs of *fhs* for formyltetrahydrofolate synthetase (FTHFS), *folD* for bifunctional formyltetrahydrofolate cyclohydrolase/methylenetetrahydrofolate dehydrogenase (FolD), *ftcD* for formimidoyltetrahydrofolate cyclodeaminase (FTCD), *metF* and *metV* for large and small subunits of 5,10-methylenetetrahydrofolate reductase (MetFV), and *acsABCDE* for the subunits of the bifunctional carbon monoxide dehydrogenase/acetyl-CoA synthase (CODH/ACS) (Fig. 4; Table S5). The absence of the acetyl-CoA synthetase (*acs*) of acetate-oxidizing sulfate reducers and the presence of phosphotransacetylase (*pta*) and acetate kinase (*ack*), which are commonly used for energy conservation in acetate-producing sulfate reducers and homoacetogenic bacteria (Table S4, S5), indicate that the pathway operates in the reductive direction.

The strongest argument for a reductive acetyl-CoA pathway in '*Ca.* Adiutrix intracellularis', however, is the presence of gene sets coding for two hydrogen-dependent CO_2 reductases (HDCR, Fig. 4; Fig. 5), the key enzyme for the hydrogenation of CO_2 to formate in the homoacetogenic bacterium *Acetobacterium woodii* (Schuchmann and Müller, 2014). Like other homoacetogens, such as *Treponema primitia* (Matson et al., 2010) and *A. woodii* (Poehlein et al., 2013), the genome of strain Adiu1 contains two separate gene clusters of HDCR components, which include the genes for a selenium-free and a selenium-containing variant of a putative formate dehydrogenase H (*fdhF1* and *fdhF2*), a gene encoding the large subunit of an [FeFe] hydrogenase (*hydA2*), and three genes (*hycB1/2/3*) for the small electron transfer subunits of the complex, each following one of the genes for the large subunits. The

208 *fdhF2* homolog contains the in-frame stop codon TGA involved in the incorporation of

209 selenocysteine (Sec) into proteins (Zinoni et al., 1987).

210 The capacity for homoacetogenesis is unusual among *Deltaproteobacteria* and has been

211 demonstrated so far only for the sulfate-reducing *D. phosphitoxidans* grown in the absence of

212 sulfate (Schink et al., 2002). Most of the genes for the Wood-Ljungdahl pathway in the

213 genome of strain Adiu1 are most similar to those in the most closely related sulfate-reducing

214 *Deltaproteobacteria* (Fig. 4), which either oxidize acetate to CO_2 (*Dg. anilini* and *Da. baarsii*;

215 Schnell et al., 1989; Widdel and Bak, 1992) or are homoacetogenic (*D. phosphitoxidans*;

216 Schink et al., 2002). By contrast, the homologs of the entire HDCR modules show the highest

217 similarities to those of homoacetogenic *Spirochaetes* and *Firmicutes* (Fig. 4; Table S5). This

218 suggests that '*Ca.* Adiutrix intracellularis' acquired the capacity for homoacetogenesis by

219 lateral gene transfer.

220 ***Energy conservation***

221 Homoacetogens maximize the production of reduced ferredoxin using [FeFe] hydrogenases

222 that couple the endergonic reduction of ferredoxin with the exergonic reduction of NAD^+

223 (electron bifurcation; see Schuchmann and Müller, 2014). The genome of strain Adiu1

224 possesses two gene cassettes (*hydABC* and *hndABC*; Table S5), which encode homologs of

225 soluble, electron-bifurcating [FeFe] hydrogenases in *Moorella thermoacetica* (HydABC;

226 Wang et al., 2013) and *A. woodii* (HydABCD; Schuchmann and Müller, 2012) that catalyze

227 the concomitant reduction of ferredoxin and NAD^+ with 2 H_2, and an $NADP^+$-dependent

228 [FeFe] hydrogenase from *Desulfovibrio fructosovorans* (HndABCD; Malki et al., 1995),

229 respectively. Both gene sets show highest sequence similarities to their homologs in

230 homoacetogenic firmicutes (*Sporomusa ovata*, *Acetonema longum*), and in the case of

231 *hndABC*, also the homoacetogenic *T. primitia* (Table S5).

232 The energetic coupling of the Wood-Ljungdahl pathway to energy conservation in the

233 homoacetogens investigated to date involves either a membrane-bound Rnf complex

234 (homoacetogens without cytochromes; e.g., *A. woodii*) or an energy-converting hydrogenase

235 (Ech) complex (homoacetogens with cytochromes; e.g., *M. thermoacetica*). In both cases, the

236 free energy change during the oxidation of reduced ferredoxin with a more positive electron

237 acceptor (NAD^+ or H^+) is used to generate a sodium- or proton-motive force across the

238 cytoplasmic membrane (Schuchmann and Müller, 2014).

239 However, there is no evidence for the presence of an Rnf complex or an Ech-like [NiFe]

240 hydrogenase in the draft genome of strain Adiu1. The only candidate for an electrogenic

241 proton or sodium pump is encoded by a gene cluster coding for the 11 core subunits of

242 complex I (*nuoABCDHIJKLMN*), the common elements of the membrane-bound NADH-

243 ubiquinone oxidoreductase complex (Nuo), and the F_{420}-methanophenazine oxidoreductase

244 complex (Fpo). This complex has most likely evolved from [NiFe] hydrogenases that lost

245 their [NiFe] cluster and gained new functions by acquiring additional electron-transferring

246 subunits, e.g., NuoEFG or FpoFO (Moparthi and Hägerhäll, 2011). Although the gene sets

247 coding for 11-subunit complexes are present in the genomes of many bacteria and archaea,

248 their interacting partner proteins or the redox process catalyzed by the respective complex are

249 often unclear (Moparthi and Hägerhäll, 2011).

250 Notably, the genes that encode methylene-THF reductase (*metVF*) in '*Ca.* Adiutrix

251 intracellularis' are preceded by genes that encode homologues of a small protein (*mvhD*) and a

252 soluble electron-bifurcating heterodisulfide reductase (*hdrA*); while the *hdrBC* genes are on a

253 different contig (Fig. S4). The *hdrCBA-mvhD-metVF* gene cluster from the homoacetogenic

254 *M. thermoacetica* encodes a heterohexameric complex of MetFV, HdrABC and MvhD that

255 reduces methylene-THF or oxidizes NADH with benzylviologen as artificial electron

256 donor/acceptor, which led to the proposal that the complex is an electron-bifurcating enzyme

257 that depends on a second, so far unidentified electron donor/acceptor (Mock et al., 2014).

258 Inspired by the ferredoxin-oxidizing activity of the Fpo-like 11-subunit complex in

259 *Methanosaeta thermophila* (Welte and Deppenmeier, 2014) and its potential interaction with

260 heterodisulfide reductase (HdrD) in *Methanomassiliicoccales* (Lang et al., 2015), we propose

261 that the 11-subunit complex of '*Ca.* Adiutrix intracellularis' oxidizes ferredoxin and transfers

262 the reducing equivalents to the cytoplasmic HdrCBA/MvhD/MetVF complex that reduces

263 methylene tetrahydrofolate and NAD^+ in an electron-bifurcating reaction (Fig. 4). It is worth

264 noting that the same gene cluster is present also in other homoacetogens that lack Rnf and in

265 sulfate reducers that oxidize acetate via the Wood-Ljungdahl pathway (Table S5).

266 ### *Carbon metabolism*

267 The draft genome of '*Ca.* Adiutrix intracellularis' contains a complete set of genes necessary

268 for the Embden-Meyerhof pathway (EMP) (Table S5). Uptake and phosphorylation of

269 hexoses proceeds via a phosphotransferase system (PTS), which consists of single gene sets

270   for the general cytoplasmic components (*ptsIH* for Enzyme I and HPr) and the sugar-specific

271   Enzyme II complex (*manXYZW*), which has the same four-subunit structure (i.e., separate

272   *manX* and *manW* genes for the IIA and IIB domains as the mannose/glucose permease of

273   *Vibrio furnissii*; Bouma and Roseman, 1996). The presence of genes encoding glucose-6-

274   phosphate isomerase (*pgi*) and phosphomannose isomerase (*manA*) indicates that the hexose

275   6-phosphates produced by the PTS are shuttled into the EMP pathway via fructose 6-

276   phosphate (Fig. 5), but since PTS systems typically transport a number of different sugars, the

277   exact nature of the substrate(s) provided by the host remains unclear.

278   The presence of all genes required for gluconeogenesis and for the biosynthesis and

279   degradation of glycogen is in agreement with the assumption that the electron-dense

280   inclusions in the cytoplasm of '*Ca.* Adiutrix intracellularis' are glycogen granules (Fig. 3).

281   The presence of genes encoding a Na^+/alanine symporter and an alanine dehydrogenase

282   suggests that alanine can be utilized as carbon and nitrogen source.

283   A pyruvate:ferredoxin oxidoreductase (PFOR) encoded by *porABDG* connects

284   glycolysis/gluconeogenesis with the Wood-Ljungdahl pathway and intermediary metabolism

285   (Fig. 5). Pyruvate carboxylase (encoded by *pyc*), malate dehydrogenase (oxaloacetate-

286   decarboxylating, *maeA*), fumarate hydratase (*fumAB*), aspartate ammonia-lyase (*aspA*) and L-

287   aspartate aminotransferase (*aspB*) mediate between the reductive branch of the TCA cycle and

288   nitrogen metabolism (Fig. 5). Citrate is most likely produced by a *Re*-citrate synthase encoded

289   by one of the gene homologs of isopropylmalate/homocitrate/citramalate synthase, as in the

290   case of *Syntrophus aciditrophicus* (Kim et al., 2013). The oxidative branch of the TCA cycle

291   is incomplete; as in many anaerobic bacteria, the genes for 2-oxoglutarate dehydrogenase and

292   succinate dehydrogenase are absent (Fig. 5).

293   *Nitrogen fixation and ammonia assimilation*

294   The draft genome of Adiu1 contains a gene cluster encoding an (alternative) Fe-nitrogenase

295   (Anf) complex (Fig. S5). It comprises the genes for the structural proteins (*anfHDK* and

296   *anfG*), an iron-containing accessory protein (*anfO*), and an activator required for their

297   transcription (Fig. S5). It is located on the same 13.7 kb-scaffold as two genes (*glnK1* and

298   *glnK2*) encoding regulatory proteins and is similar in structure to the *nifHDK* cluster of many

299   nitrogen-fixing bacteria (Fig. S5). Homologs of genes involved in the assembly of nitrogenase

300   components and the incorporation of iron into the active center (*nifB*, *nifS*, and *nifU*) are also

301 present (Table S5). The genome contains homologs a glutamine synthetase (*glnA*) and

302 glutamate synthase (*gltBD*) for the assimilation of ammonia. The location of *glnB* homologs

303 (*glnK1* and *glnK2*) encoding for the regulatory protein P-II directly downstream of the gene

304 for the ammonia transport protein (*amt*) indicates that nitrogen metabolism in 'Ca. Adiutrix

305 intracellularis' is regulated the same way as in *Escherichia coli* (Javelle et al., 2004). The

306 iron-only cofactor (FeFeco) required by the Anf-type nitrogenase is most likely synthesized

307 by a pathway related to the biosynthesis of the molybdenum-containing cofactor (FeMoco)

308 (Yang et al., 2014), as indicated by the presence of the corresponding genes in the draft

309 genome (Table S5).

310 Phylogenetic analysis revealed that the *anfH* gene of 'Ca. Adiutrix intracellularis' belongs to a

311 termite-specific cluster of *nifH* genes that belongs to Group II nitrogenases and comprises

312 homologs of termite gut bacteria from different phyla (Fig. S6). It includes the flagellate

313 symbiont '*Ca.* Armantifilum devescovinae', one of several lineages of nitrogen-fixing

314 *Bacteroidales* (Arma Cluster II) that colonize cytoplasm and surface of termite gut flagellates

315 and cospeciate with their respective hosts (e.g., Hongoh et al., 2008a; Desai and Brune, 2012).

316 Since the primary and secondary symbionts (*Ca.* Endomicrobium and *Ca.* Desulfovibrio) of

317 *Trichonympha agilis* lack the capacity for N_2 fixation (Hongoh et al., 2008b; Sato et al.,

318 2009), the acquisition of a third symbiont by *T. collaris* may serve to complement this missing

319 function.

320 *Amino acid and cofactor biosynthesis*

321 The draft genome of Adiu1 contains almost complete gene sets for the biosynthesis of all

322 standard amino acids except asparagine (Fig. S7). The absence of asparagine synthetase

323 suggests that asparagine must be acquired from the environment, most likely via the ATP-

324 binding cassette (ABC) transporter of polar amino acids encoded by the *gln* gene cluster

325 (Table S5). The presence of the genes for lysine biosynthesis via the meso-diaminopimelate

326 pathway is in agreement with the assumption that the homolog of

327 isopropylmalate/homocitrate/citramalate synthase is not involved in amino acid biosynthesis

328 but encodes a citrate synthase (Table S4, also see Carbon metabolism). In addition, the draft

329 genome contains all genes required for the biosynthesis of selenocysteine, which is an

330 essential component of the catalytic center of FDH_H-Sec in the HDCR enzyme complex (see

331 Wood-Ljungdahl pathway). Like all other genes coding for components of this complex, also

332   *selA* and *selD* (encoding seryl-tRNA selenium transferase and selenide, water dikinase) are

333   most closely related to their homologs in *Firmicutes* (Table S5).

334   Coenzyme B_{12} is essential for both the methyl and carboxyl branches of the Wood-Ljungdahl

335   pathway. The draft genome of Adiu1 contains an almost complete set of genes required for

336   the biosynthesis of cobalamin via precorrin-2 (Table S4). 'Ca. Adiutrix intracellularis' lacks

337   the *cbiJ* gene encoding an analog of precorrin-6x reductase (CobK), as in other

338   *Deltaproteobacteria* and a number of archaea (Rodionov et al., 2004), suggesting it is

339   probably not necessary for the biosynthesis of cobalamin. The presence of a vitamin B_{12}

340   transporter (encoded by *btuBCD*; Table S5) may allow 'Ca. Adiutrix intracellularis' to

341   provide vitamin B_{12} to its host.

342   The draft genome of Adiu1 contains all genes required for the biosynthesis of riboflavin,

343   NAD, siroheme, and menaquinone (Table S5). Although the genes for the biosynthesis of

344   coenzyme A from pantothenate are present, the pathway leading to this precursor seems to be

345   absent. Also the genes involved in the biosynthesis of biotin and tetrahydrofolate (THF) are

346   absent or incomplete, respectively, suggesting that the endosymbiont depends on the external

347   supply of these compounds. A requirement for THF precursors in a homoacetogen is not

348   unprecedented; also *T. primitia* depends on the cross-feeding of 5'-formyl-THF by other gut

349   bacteria in the termite guts (Graber and Breznak, 2005).

350   ***Ecology and evolution***

351   Reductive acetogenesis from H_2 and CO_2 is the major hydrogen sink in the hindgut of wood-

352   feeding termites, and there is a large body of evidence for a major role of spirochetes in this

353   process, which typically form a large proportion of the bacterial microbiota of wood-feeding

354   species (see reviews by Breznak, 2000; Breznak and Leadbetter, 2006; Brune, 2014). After the

355   isolation of *T. primitia*, the first representative of the phylum Spirochaetes that was capable of

356   reductive acetogenesis (Leadbetter et al.,1999; Graber and Breznak, 2004), numerous studies

357   have documented the importance of related lineages from the *Treponema* I clade in termite

358   guts based on diversity and expression profiles of phylogenetic and functional marker genes

359   or on metagenomic approaches (e.g., Ottesen et al., 2006; Pester and Brune 2006; Warnecke

360   et al., 2007; Zhang et al., 2011).

361   Therefore, it was quite surprising when Rosenthal et al. (2013) reported that spirochetes may

362   not be the only organisms that contribute importantly to reductive acetogenesis is termite guts.

363 Using microfluidic multiplex digital PCR, they showed that the two most abundant *fdhF* gene

364 transcripts in the gut of *Zootermopsis nevadensis* belong to an uncultured

365 deltaproteobacterium (phylotype ZnDP-F1, JX974519) with 99.9% sequence similarity to the

366 16S rRNA gene of '*Ca.* Adiutrix intracellularis', and documented that cells of this phylotype

367 are associated with *Trichonympha* flagellates (Rosenthal et al., 2013). The sequences of

368 clones ZnHcys (GQ922420) and ZnD2sec (GU563467) encode a cysteine-dependent and

369 selenocysteine-dependent variant of formate dehydrogenase H (a component of HDCR) and

370 are almost identical (99%) to the nucleotide sequences of *fdhF1* and *fdhF2* in the Adiu1

371 genome. Although the authors reported that the cells of ZnDP-F1 phylotype were associated

372 with the surface of the protist, their images would be also consistent with an intracellular

373 location. Therefore, it seems safe to conclude that the deltaproteobacterial symbiont of

374 *Trichonympha* flagellates reported by Rosenthal et al. (2013) is identical to '*Ca.* Adiutrix

375 intracellularis'.

376 Reductive acetogenesis is quite unusual for *Deltaproteobacteria*, but our genome analysis of

377 '*Ca.* Adiutrix intracellularis' corroborates these exciting findings by documenting the

378 presence of the full set of genes required for reductive homoacetogenesis. In addition, it sheds

379 light on the evolutionary origin of the homoacetogenic capacity in this novel lineage of

380 *Deltaproteobacteria*, which apparently complemented an existing Wood-Ljungdahl pathway

381 by acquiring a few key genes encoding HDCR from other bacterial lineages, most likely by

382 lateral gene transfer. It is an intriguing question whether this metabolic change happened in an

383 ancestral member of the Rs-K70 cluster, which would imply that the entire order-level cluster

384 is homoacetogenic. However, it is also possible that the putatively free-living relatives of '*Ca.*

385 Adiutrix intracellularis' present in other insects are still sulfate reducers, and the gene transfer

386 rendering them homoacetogenic was a more recent event – and possibly a prerequisite for

387 colonization of the intracellular habitat. The very recent report of a homoacetogenic

388 spirochete as an endosymbiont of a different gut flagellate in another termite species (Ohkuma

389 et al., 2015) suggests that the capacity for reductive acetogenesis may indeed facilitate the

390 colonization of the cytoplasm of termite gut flagellates members of various phyla.

391 The retention of the biosynthetic pathways for nitrogen fixation and the synthesis of most

392 amino acids and vitamins in the genome of '*Ca.* Adiutrix intracellularis' matches previous

393 reports on other flagellate endosymbionts (Hongoh et al., 2008a, 2008b, Ohkuma et al., 2015).

394 There is general agreement on the hypothesis that such intracellular symbioses have a

395 nutritional basis (McCutcheon and Moran, 2012). Nitrogen fixation may be the evolutionary

396 driver in the association with bacterial ectosymbionts of gut flagellates in dry-wood termites

397 (Desai and Brune, 2012) – a hypothesis that can possibly be extended to any other

398 associations where the bacteria colonizing the cell surface are exploited as nutrient source via

399 phagocytosis and subsequent digestion (see Brune, 2014). In the case of endosymbionts,

400 however, the exchange of nutrients with the host cell is not a trivial issue. The number of

401 ABC transporters in the genome of '*Ca.* Adiutrix intracellularis' is larger than found, e.g., in

402 the primary endosymbionts of insects (Charles et al., 2015) and includes several homologs

403 putatively involved in the transport of ions or amino acids (Table S4), which may serve to

404 mediate metabolite transfer between symbiont and host.

405 The capacity for reductive acetogenesis in an endosymbiont is highly unusual and has been

406 found only in the recently discovered '*Candidatus* Treponema intracellularis', whose cells are

407 located close to the hydrogenosomes in the cytoplasm of *Eucomonympha* flagellates in the

408 dampwood termite *Hodotermopsis sjoestedti* (Ohkuma et al., 2015). In view of the extremely

409 high hydrogen partial pressures in the hindgut of *Zootermopsis nevadensis* (Pester and Brune,

410 2007), it is not clear whether the proximity to the hydrogen source is required to maintain

411 high rates of hydrogen transfer or whether it is merely based on the abundant presence of the

412 organelles in the posterior cell region. Also the reasons for the close situation of '*Ca.* Adiutrix

413 intracellularis' to '*Ca. Desulfovibrio trichonymphae*' in the anterior cell region and its

414 consequences are open to speculation. Although the metagenome library of the flagellate

415 symbionts did not provide sufficient information to fully reconstruct the metabolism of the

416 '*Ca. Desulfovibrio trichonymphae*', a provisional analysis of the gene content indicates that

417 this symbiont is a sulfate reducer (Fig. 4) and shows high similarities to the sequences in the

418 genomes of two undescribed *Desulfovibrio* species (strains 3_1_syn3 and 6_1_46AFAA)

419 isolated from the human gut (BioProject accession No.: PRJNA42529 and PRJNA40021,

420 respectively).

421 The extracellular location of 'Ca. *Desulfovibrio trichonymphae*' on the surface of *T. collaris*

422 may reflect the need for a provision with sulfate via the gut fluid. Interestingly, cells of the

423 related phylotype of '*Ca. Desulfovibrio* trichonymphae' associated with *Trichonympha*

424 *globulosa* from *Incisitermes marginipennis* are embedded much deeper into invaginations of

425 the cell surface but maintain a connection to the exterior of the host cell (Strassert et al, 2012),

426 whereas cells of '*Ca. Desulfovibrio* trichonymphae' associated with *Trichonympha agilis* from

427   *Reticulitermes speratus* seem to be true endosymbionts that are completely surrounded by a

428   host membrane (Sato et al., 2009). The consequences of the location for the provision of the

429   symbionts with sulfate are not clear, but the switch to a homoacetogenic metabolism in '*Ca.*

430   Adiutrix intracellularis' may be enforced by a lack of sulfate in its intracellular habitat.

431   ***Description of* 'Candidatus *Adiutrix intracellularis'***

432   'Adiutrix intracellularis' (Ad.iu'trix in'tra.cel.lu.la'ris. L. f. n. *adiutrix*, a female helper or

433   assistant; L. prep. *intra*, within; L. fem. dim. n. *cellula*, a small chamber or cell; L. fem.

434   suff. -*aris*, suffix denoting pertaining to; N.L. fem. adj. *intracellularis*, intracellular; *Adiutrix*

435   *intracellularis*, an intracellular symbiont.

436   Properties: Rod-shaped bacteria (approximately 0.5–0.6 in diameter and 0.8–1.9 μm in length)

437   with slightly pointed ends. Form a monophyletic group with the SSU rRNA genes of other

438   *Deltaproteobacteria* from termite guts. Possesses genes encoding for production of acetate

439   from CO_2 and H_2 (Wood–Ljungdahl pathway) and dinitrogen fixation. Colonize the cytoplasm

440   of the parabasalid flagellate *Trichonympha collaris* in the hindgut of the termite *Zootermopsis*

441   *nevadensis*.

442   So far uncultured. The basis of assignment are the SSU rRNA gene sequences of

443   representative phylotypes (Accession No. AB972401; AB894435–AB894480) and

444   hybridization with the specific SSU rRNA-targeted oligonucleotide probe Delta-Tr3-Zn (5'-

445   CTT GAA CCG AAG TTC CTG -3'). A draft genome of strain Adiu1, reconstructed from

446   metagenome sequences, has been deposited in the Integrated Microbial Genomes (IMG)

447   database (IMG Genome ID: 2556793040) and GenBank database (pending).

448

449   **Experimental procedures**

450   *Insects*

451   Termites were the same as in previous studies (Ikeda-Ohtsubo et al., 2007; Ikeda-Ohtsubo and

452   Brune, 2009; Desai et al., 2010). Colonies were maintained in the laboratory on a diet of

453   pinewood; only pseudergates (workers) were used in the experiments. Cockroaches and

454   *Pachnoda ephippiata* larvae were obtained from commercial breeders (Dietrich et al., 2014).

455   Insects were dissected and hindgut DNA was extracted as previously described (Ikeda-

456   Ohtsubo et al., 2007).

457   *Cloning and sequencing of 16S rRNA genes*

458   The 16S rRNA genes of uncultured *Deltaproteobacteria* were amplified using the forward

459   primer UncDelta234F [5′-(A/G)GCC(C/T)GCGTGACATTAGAT(T/A)GAT-3′], which was

460   designed to exclusively match all members of the Rs-K70 lineage identified in previous

461   studies, and the general bacteria primer Bact1389R (5′-ACGGGCGGTGTGTACAAG-3′;

462   Osborn et al., 2000). The PCR conditions involved an initial denaturation step of 3 min at

463   94 °C, 32 cycles of 30 s at 94 °C, 30 s at 66.6 °C, and 45 s at 72 °C, and a final extension step

464   of 7 min at 72 °C. All reactions yielded amplicons of the expected length (~1,150 bp), which

465   were cloned and sequenced as previously described (Ikeda-Ohtsubo et al., 2007). SSU rRNA

466   gene sequences obtained in this study have been deposited at GenBank under accession

467   numbers AB894435–53, AB894461–80, and AB972401.

468   *Phylogenetic analysis*

469   Sequences in this study were imported and aligned against a curated reference database of

470   16S rRNA genes based on the Silva database (release 119) and including all sequences

471   previously obtained from termites and cockroaches (Mikaelyan et al., 2015). Sequences were

472   analyzed using the tools implemented in the *ARB* software package (Ludwig et al., 2004).

473   Highly variable columns were removed from the alignment using base frequency (< 50%

474   identical bases), and phylogenetic trees were calculated under the maximum-likelihood

475   criterion using *RAxML* with the GTR+Γ+I model and 1,000 bootstrap replicates.

476   *FISH analysis*

477   Fixation of hindgut contents, *in situ* hybridization, washing steps, and epifluorescence

478   microscopy were performed as previously described (Ikeda-Ohtsubo and Brune, 2009). For

479   the specific detection and localization of '*Ca.* Adiutrix intracellularis', we used a newly

480   designed oligonucleotide probe (Delta-ZnvTr3; 5′-CTT GAA CCG AAG TTC CTG-3′) that

481   was specific for all phylotypes of '*Ca.* Adiutrix intracellularis' and a probe (ALF968; Neef et

482   al., 1998) that targeted a wide range of *Proteobacteria* but had one significant mismatch to

483   16S rRNA of *Desulfovibrio* species. '*Ca.* Desulfovibrio trichonymphae' was localized using a

484   previously published *Desulfovibrio* probe (DSV698; Manz et al., 1998). The probes exactly

485   matched the SSU rRNA gene sequences of their respective targets and had at least two

486   mismatches to any other clones obtained from the *Trichonympha* suspensions of *Z. nevadensis*

487   (Strassert et al., 2012; this study). *T. collaris* cells were identified with a species-specific

488   probe (ZTcA-Euk; Ikeda-Ohtsubo, 2007). For all probes, formamide was included at

489   concentrations that were optimized for stringent hybridization conditions (20% for probe

490   Delta-ZnvTr3, all others as previously published).

491   *Electron microscopy*

492   The contents of two termite hindguts were suspended in Solution U (Trager, 1934).

493   Approximately 120 flagellates identified as *Trichonympha collaris* were collected by

494   micropipetting and fixed in 2.5% glutaraldehyde in 50 mM Soerensen phosphate buffer. Prior

495   to further treatments, the sample was stored overnight at 4 °C. After three rinses in 50 mM

496   cacodylate buffer, the flagellates were post-fixed for 2 h in reduced osmium tetroxide (2%

497   OsO_4 plus 3% $K_4[Fe(CN)_6]$, mixed 1:1; Karnovsky, 1971). After three further rinses in 50

498   mM cacodylate buffer, the flagellates were dehydrated in an increasing series of ethanol and

499   embedded in Spurr's resin (1969). Ultrathin sections were stained with saturated uranyl

500   acetate and lead citrate according to Reynolds (1963) and examined with a Philips EM 208

501   transmission electron microscope.

502   *Preparation of symbiont DNA for metagenome sequencing*

503   Hindgut fluid of ~250 individuals of *Z. nevadensis* was collected in a 2-ml centrifuge tube and

504   gently mixed with 1.2 ml ice-cold Solution U. After about 10 min, the *Trichonympha* cells

505   had sedimented at the bottom of the tube. The supernatant was removed with a micropipette

506   and replaced with fresh solution U. After five such washing steps, the cells were resuspended

507   in isolation buffer (Prechtl et al., 2004) and disrupted using ultrasonication (UP50H,

508   Hielscher, Teltow, Germany; 1-mm tip, 10 cycles of 0.5 s at 30% amplitude).

509   After removal of flagellate cell debris by centrifugation at $500 \times g$ for 2 min, the supernatant

510   was homogenized by pressing it twice through an 18-gauge syringe needle and then filtered

511   through an 80-μm nylon mesh mounted in a Swinex filter holder (Millipore) to remove

512   remaining cell debris and wood particles. The filtrate was treated with DNaseI (RQ1 DNase,

513   Promega) for 15 min to digest flagellate DNA, which dissolved remaining cell aggregates,

514   and subsequently filtered through a 20-μm nylon mesh (Swinex filter holder), and membrane

515   filters of 5-µm and 0.65-µm pore size (Ultrafree-CL centrifugal filter tubes, Amicon). The

516   bacterial cells in the filtrate were sedimented by centrifugation at $8,000 \times g$ for 20 min and

517   resuspended in PBS buffer (130 mM NaCl, 7 mM Na_2HPO_4 and 3 mM NaH_2PO_4, pH 7.4). All

518   procedures were conducted either on ice or at 4 °C.

519   The cell suspension was kept at 65 °C for 10 min to inactivate DNase I, centrifuged again, and

520   resuspended in TE buffer (10 mM Tris-HCl, 1 mM EDTA, pH 8.0). DNA extraction followed

521   a previously described procedure (Herlemann et al., 2009) and yielded 12 µg of high-

522   molecular-weight (>23 kb) DNA.

523   *Metagenome sequencing and assembly*

524   The DNA of the bacterial symbionts was used to construct both a 16S rRNA gene library and

525   a metagenomic library. The 16S rRNA gene library was constructed and sequenced at the

526   Joint Genome Institute (JGI) following previously described procedures (Warnecke et al.,

527   2007). The resulting sequences were aligned with their closest relatives in our reference

528   database (DictDb; Mikaelyan et al., 2015) and classified into different taxa (Fig. S1). Also the

529   metagenomic DNA was sequenced at the JGI using a combination of Sanger sequencing of a

530   short-insert library and 454-GS20 pyrosequencing following standard procedures. 454

531   sequences were assembled with Newbler then "shredded" into Sanger-like reads that were

532   coassembled with the Sanger data using the Paracel Genome Assembler (pga;

533   www.paracel.com).

534   The original metagenome assembly (GOLD ID: Gp0051377, NCBI BioProject accession:

535   PRJNA78659) consisted of 24.9 Mbp of metagenome data in 22,673 scaffolds. Scaffolds with

536   a length of more than 1,000 bp (11.9 Mb, 4,237 scaffolds) were classified using PhyloPythiaS

537   (Patil et al., 2012; Gregor et al. 2014), which yielded 13 phylogenetic groups (Table S1). The

538   training data included generic models representing all clades of bacteria and sample-specific

539   generic models for the major bacterial symbionts identified in the 16S rRNA gene library

540   obtained from the same DNA preparation (Table S1). As specific training data for '*Ca.*

541   Adiutrix intracellularis', we selected several large scaffolds (~100 kb in total) that contained

542   either the SSU rRNA gene of Adiu1 or single-copy phylogenetic marker genes of

543   *Deltaproteobacteria* other than *Desulfovibrionaceae*.

544   In addition to the 144 scaffolds assigned to '*Ca.* Adiutrix intracellularis', we identified 11

545   scaffolds using a combination of the following criteria: (i) the average G+C content was

546   closer to that of *bona fide* Adiu1 sequences (43.3 %) than to sequences of '*D.*

547   *trichonymphae*'(55 %), (ii) the coding sequences (CDS) in the scaffold had the highest

548   similarity to genes of *Deltaproteobacteria* species in the GenBank database and were more

549   similar to *Desulfobacterium*, *Syntrophobacter*, or *Desulfobacca* spp. than to *Desulfovibrio*

550   spp., and (iii) the scaffolds did not contain CDS with a high similarity to other bacterial

551   lineage represented in the 16S rRNA gene library (Table S1). Scaffolds matching these criteria

552   were further validated by verifying the phylogenetic position of least one CDS in the scaffold

553   using BLASTP (http://blast.ncbi.nlm.nih.gov).

554   The resulting draft genome of strain Adiu1 was uploaded to the Integrated Microbial

555   Genomes Expert Review (IMG-ER) platform (Markowitz et al, 2009), where gene-calling and

556   automatic functional annotation were performed. Metabolic reconstruction of Adiu1 was

557   performed based on a list of functional genes involved in important metabolic pathways

558   (Table S2), each of which were automatically and then manually curated by comparing the

559   predicted protein sequences with those in GenBank and IMG databases. The final annotation

560   of the draft genome of '*Ca.* Adiutrix intracellularis' strain Adiu1 (IMG Genome ID:

561   2556793040) has been submitted to Genbank (pending).

References

574

575 Bouma, C.L., and Roseman, S. (1996) Sugar transport by the marine chitinolytic bacterium

576   *Vibrio furnissii*. Molecular cloning and analysis of the mannose/glucose permease. *J Biol*

577   *Chem* **271:** 33468–33475.

578 Breznak, J.A. (2000) Ecology of prokaryotic microbes in the guts of wood- and litter-feeding

579   termites. In *Termites: Evolution, Sociality, Symbiosis, Ecology*. Abe, T., Bignell, D. E.

580   and Higashi, M. (eds). Dordrecht: Kluwer, pp. 209–231.

581 Breznak, J.A., and Leadbetter, J.R. (2006) Termite gut spirochetes. In *The Prokaryotes, 3rd*

582   *edn., Vol. 7*. Dworkin, M., Falkow, S., Rosenberg, E., Schleifer, K-H., and Stackebrandt,

583   E. (eds). New York, NY, USA: Springer, pp. 318–329.

584 Brugerolle, G., and Radek, R. (2006) Symbiotic protozoa of termites. In *Intestinal*

585   *Microorganisms of Termites and Other Invertebrates*. König, H., and Varma, A. (eds).

586   Berlin: Springer, pp. 243–269.Brune, A. (2014) Symbiotic digestion of lignocellulose in

587   termite guts. *Nat Rev Microbiol* **12:** 168–180.

588 Brune, A., and Ohkuma, M. (2011) Role of the termite gut microbiota in symbiotic digestion.

589   In *Biology of Termites: A Modern Synthesis*. Bignell, D.E., Roisin, Y., and Lo, N. (eds).

590   Dordrecht: Springer, pp. 439–475.

591 Charles, H., Balmand, S., Lamelas, A., Cottret, L., Pérez-Brocal, V., Burdin, B., et al. (2015)

592   A genomic reappraisal of symbiotic function in the aphid/*Buchnera* symbiosis: reduced

593   transporter sets and variable membrane organisations. *PLoS One* **6:** e29096.

594 Cleveland, L.R. (1925) The ability of termites to live perhaps indefinitely on a diet of pure

595   cellulose. *Biol Bull* **48:** 289–293.

596   Carpenter, K.J., Chow, L., and Keeling, P.J. (2009) Morphology, phylogeny, and diversity of

597   *Trichonympha* (Parabasalia: Hypermastigida) of the wood-feeding cockroach

598   *Cryptocercus punctulatus*. J Eukaryot Microbiol **56**: 305–313.

599   Desai, M.S., Strassert, J.F.H., Meuser, K., Hertel, H., Ikeda-Ohtsubo, W., Radek, R., and

600   Brune, A. (2010) Strict cospeciation of devescovinid flagellates and *Bacteroidales*

601   ectosymbionts in the gut of dry-wood termites (*Kalotermitidae*). *Environ Microbiol* **12:**

602   2120–2132.

603   Desai, M.S., and Brune, A. (2012) *Bacteroidales* ectosymbionts of gut flagellates shape the

604   nitrogen-fixing community in dry-wood termites. *ISME J* **6**: 1302–1313.

605   Dietrich, C., Köhler, T., and Brune, A. (2014) The cockroach origin of the termite gut

606   microbiota: patterns in bacterial community structure reflect major evolutionary events.

607   *Appl Environ Microbiol* **80:** 2261–2269.

608   Fröhlich, J., Sass, H., Babenzien, H.-D., Kuhnigk, T., Varma, A., Saxena, S., et al. (1999)

609   Isolation of *Desulfovibrio intestinalis* sp. nov., from the hindgut of the lower termite

610   *Mastotermes darwiniensis*. *Can J Microbiol* **45**: 145–152.

611   Garcia Martin, H., Ivanova, N., Kunin, V., Warnecke, F., Barry, K.W., et al. (2006)

612   Metagenomic analysis of two enhanced biological phosphorus removal (EBPR) sludge

613   communities. *Nat Biotechnol* **24:** 1263–1269.

614   Graber, J.R., and Breznak, J.A. (2004) Physiology and nutrition of *Treponema primitia*, an

615   H_2/CO_2-acetogenic spirochete from termite hindguts. *Appl Environ Microbiol* **70:** 1307–

616   1314.

617   Graber, J.R., and Breznak, J.A. (2005) Folate cross-feeding supports symbiotic

618   homoacetogenic spirochetes. *Appl Environ Microbiol* **71:** 1883–1889.

619   Gregor, I., Dröge, J., Schirmer, M., Quince, C., and McHardy, A.C. (2014) PhyloPythiaS+: A

620   self training method for the rapid reconstruction of low-ranking taxonomic bins from

621   metagenomes. *ArXiv e-prints* 1–48.

622   Herlemann, D.P.R., Geissinger, O., Ikeda-Ohtsubo, W., Kunin, V., Sun, H., Lapidus, A.,

623   Hugenholtz, P., and Brune, A. (2009) Genomic analysis of "*Elusimicrobium minutum*,"

624   the first cultivated representative of the phylum "*Elusimicrobia*" (formerly Termite Group

625   1). *Appl Environ Microbiol* **75**: 2841–2849.

626   Hongoh, Y., and Ohkuma, M. (2010) Termite gut flagellates and their methanogenic and

627   eubacterial symbionts. In *(Endo)symbiotic Methanogenic Archaea*. Hackstein, J.H.P. (ed).

628   Heidelberg: Springer, pp. 55–79.

629   Hongoh, Y., Ohkuma, M., and Kudo, T. (2003). Molecular analysis of bacterial microbiota in

630   the gut of the termite *Reticulitermes speratus* (Isoptera, Rhinotermitidae). *FEMS*

631   *Microbiol Ecol* **44**: 231–242.

632   Hongoh, Y., Deevong, P., Inoue, T., Moriya, S., Trakulnaleamsai, S., Ohkuma, M.,

633   Vongkaluang, C., Noparatnaraporn, N., and Kudo, T. (2005) Intra- and interspecific

634   comparisons of bacterial diversity and community structure support coevolution of gut

635   microbiota and termite host. *Appl Environ Microbiol* **71**: 6590–6599.

636   Hongoh, Y., Sharma, V.K., Prakash, T., Noda, S., Toh, H., Taylor, T.D., et al. (2008a) Genome

637   of an endosymbiont coupling N_2 fixation to cellulolysis within protist cells in termite gut.

638   *Science* **322**: 1108–1109.

639   Hongoh, Y., Sharma, V.K., Prakash, T., Noda, S., Taylor, T.D., Kudo, T., et al. (2008b)

640   Complete genome of the uncultured Termite Group 1 bacteria in a single host protist cell.

641   *Proc Natl Acad Sci USA* 105: 5555–5560.

642   Hungate, R.E. (1943) Quantitative analysis on the cellulose fermentation by termite protozoa.

643   *Ann Entomol Soc Am* **36:** 730–739.

644   Ikeda-Ohtsubo, W. (2007) *Endomicrobia* in termite guts: symbionts within a symbiont.

645   Phylogeny, cospeciation with host flagellates, and preliminary genome analysis.

646   Dissertation, Philipps-Universität Marburg, Germany.

647   Ikeda-Ohtsubo, W., and Brune, A. (2009) Cospeciation of termite gut flagellates and their

648   bacterial endosymbionts: *Trichonympha* species and '*Candidatus* Endomicrobium

649   trichonymphae'. *Mol Ecol* **18**: 332–342.

650   Ikeda-Ohtsubo, W., Desai, M., Stingl, U., and Brune. A. (2007) Phylogenetic diversity of

651   "*Endomicrobia*" and their specific affiliation with termite gut flagellates. *Microbiology*

652   **153:** 3458–3465.

653   Ikeda-Ohtsubo, W., Faivre, N., and Brune, A. (2010) Putatively free-living "Endomicrobia" –

654   ancestors of the intracellular symbionts of termite gut flagellates? *Environ Microbiol Rep*

655   **2**: 554–559.

656   Javelle, A., Serveri, E., Thornton, J., and Merrick, M. (2004) Ammonium sensing in

657   *Escherichia coli*: role of the ammonium transporter AmtB and AmtB-GlnK complex

658   formation. *J Biol Chem* **279:** 8530–8538.

659   Karnovsky, M.J. (1971) Use of ferrocyanide-reduced osmium tetroxide in electron

660   microscopy. Abstract 284. In *Proceedings of the 11th Annual Meeting of the American*

661   *Society for Cell Biology*. New Orleans, p. 146.

662   Kim, M., Le, H., McInerney, M.J., and Buckel, W. (2013) Identification and characterization

663   of *Re*-citrate synthase in *Syntrophus aciditrophicus*. *J Bacteriol* **195:** 1689–1696.

664   Kirby, H. Jr (1932) Flagellates of the genus *Trichonympha* in termites. *Univ Calif Publ Zool*,

665   **37**: 349–476.

666   Köhler, T., Dietrich, C., Scheffrahn, R.H., and Brune, A. (2012) High-resolution analysis of

667   gut environment and bacterial microbiota reveals functional compartmentation of the gut

668   in wood-feeding higher termites (*Nasutitermes* spp.). *Appl Environ Microbiol* **78**: 4691–

669   4701.

670   Kuever, J. (2014) The Family Desulfobacteraceae. In *The Prokaryotes, Vol. 10:*

671   *Deltaproteobacteria* and *Epsilonproteobacteria*. Berlin: Springer, pp. 45–73.

672   Kuhnigk, T., Branke, J., Krekeler, D., Cypionka, H., and König, H. (1996) A feasible role of

673   sulfate-reducing bacteria in the termite gut. *Syst Appl Microbiol* **19**: 139–149.

674   Lang, K., Schuldes, J., Klingl, A., Poehlein, A., Daniel, R., and Brune, A. (2015) New mode

675   of energy metabolism in the seventh order of methanogens as indicated by comparative

676   genome analysis of "*Candidatus* Methanoplasma termitum". *Appl Environ Microbiol* **81:**

677   1338–1352.

678   Leadbetter, J. R., Schmidt, T. M., Graber, J. R., and Breznak, J. A. (1999) Acetogenesis from

679   H_2 plus CO_2 by spirochetes from termite guts. *Science* **283:** 686–689.

680   Lee, M. J., Schreurs, P. J., Messer, A.C., and Zinder, S.H. (1987) Association of methanogenic

681   bacteria with flagellated protozoa from a termite hindgut. *Curr Microbiol* **15**: 337–341.

682   Leidy, J. (1881) The parasites of the termites. *J Acad Nat Sci Philadelphia 2nd Ser* **8**: 425–

683   447.

684   Ljungdahl, L.G. (1994) The acetyl-CoA pathway and the chemiosmotic generation of ATP

685   during acetogenesis. In *Acetogenesis*. Ferry, J.G. (eds). New York, NY, USA: Chapman

686   & Hall, pp. 63–87.

687   Ludwig, W., Strunk, O., Westram, R., Richter, L., Meier, H., Yadhukumar, et al. (2004) ARB:

688   a software environment for sequence data. *Nucleic Acids Res* **32**: 1363–1371.

689 Manz, W., Eisenbrecher, M., Neu, T.R., and Szewzyk, U. (1998) Abundance and spatial

690   organization of Gram-negative sulfate-reducing bacteria in activated sludge investigated

691   by in situ probing with specific 16S rRNA targeted oligonucleotides. *FEMS Microbiol*

692   *Ecol* **25**: 43–61.

693 Markowitz, V.M., Ivanova, N.N., Chen, I.M., Chu, K., and Kyrpides, N.C. (2009) IMG ER: a

694   system for microbial genome annotation expert review and curation. *Bioinformatics* **25**:

695   2271–2278.

696 Malki, S., Saimmaine, I., De Luca, G., Rousset, M., Dermoun, Z. and Belaich, J.P. (1995)

697   Characterization of an operon encoding an NADP-reducing hydrogenase in *Desulfovibrio*

698   *fructosovorans*. *J Bacteriol* **177:** 2628–2636.

699 Matson, E.G., Zhang, X., and Leadbetter, J.R. (2010) Selenium controls transcription of

700   paralogous formate dehydrogenase genes in the termite gut acetogen, *Treponema*

701   *primitia*. *Environ Microbiol* **12**: 2245–2258.

702 McCutcheon, J.P., and Moran, N.A. (2012) Extreme genome reduction in symbiotic bacteria.

703   *Nat Rev Microbiol* **10:** 13–26.

704 Messer, A.C., and Lee, M.J. (1989) Effect of chemical treatments on methane emission by the

705   hindgut microbiota in the termite *Zootermopsis angusticollis*. *Microb Ecol* **18**: 275–284.

706 Mikaelyan, A., Köhler, T., Lampert, N., Rohland, J., Boga, H., Meuser, K., and Brune, A.

707   (2015) Classifying the bacterial gut microbiota of termites and cockroaches: a curated

708   phylogenetic reference database (DictDb). Syst Appl Microbiol,

709   http://dx.doi.org/10.1016/j.syapm.2015.07.004.

710 Mock, J., Wang, S., Huang, H., Kahnt, J., and Thauer, R.K. (2014) Evidence for a

711   hexaheteromeric methylenetetrahydrofolate reductase in *Moorella thermoacetica*. *J*

712   *Bacteriol* **196:** 3303–3314

713 Moparthi, V.K., and Hägerhäll, C. (2011) The evolution of respiratory chain complex I from a

714   smaller last common ancestor consisting of 11 protein subunits. *J Mol Evol* **72:** 484–497

715 Moran, N.A., McCutcheon, J.P., and Nakabachi, A. (2008). Genomics and evolution of

716   heritable bacterial symbionts. *Ann Rev Genetics* **42**: 165–190.

717 Neef, A., Amann, R., Schlesner, H., and Schleifer, K.-H. (1998) Monitoring a widespread

718   bacterial group: in situ detection of planctomycetes with 16S rRNA-targeted probes.

719   *Microbiology* **144**: 3257–3266.

720 Noda, S., Ohkuma, M., Usami, R., Horikoshi, K., and Kudo, T. (1999) Culture-independent

721   characterization of a gene responsible for nitrogen fixation in the symbiotic microbial

722   community in the gut of the termite *Neotermes koshunensis*. *Appl Environ Microbiol* **65:**

723   4935–4942.

724 Noda, S., Hongoh, Y., Sato, T., and Ohkuma, M. (2009) Complex coevolutionary history of

725   symbiotic Bacteroidales bacteria of various protists in the gut of termites. *BMC Evol Biol*

726   **9:** 158.

727 Ohkuma, M., and Brune, A. (2011) Diversity, structure, and evolution of the termite gut

728   microbial community. In *Biology of Termites: A Modern Synthesis*. Bignell, D.E., Roisin,

729   Y., Lo, N. (eds). Dordrecht: Springer, pp. 413–438.

730 Ohkuma, M., Iida, T., Ohtoko, K., Yuzawa, H., Noda, S., Viscogliosi, E., and Kudo, T. (2005)

731   Molecular phylogeny of parabasalids inferred from small subunit rRNA sequences, with

732   emphasis on the *Hypermastigea*. *Mol Phylogenet Evol* **35**: 646–655.

733 Ohkuma, M., Noda, S., Hongoh, Y., Nalepa, C.A., Inoue, T. (2009) Inheritance and

734   diversification of symbiotic trichonymphid flagellates from a common ancestor of

735   termites and the cockroach *Cryptocercus*. Proc R Soc B **276:** 239–245.

736 Ohkuma, M., Noda, S., Hattori, S., Iida, T., Yuki, M., Starns, D., Inoue, J.-I., Darby, A.C.,

737   Hongoh, Y. (2015) Acetogenesis from H_2 plus CO_2 and nitrogen fixation by an

738   endosymbiotic spirochete of a termite-gut cellulolytic protist. *Proc Natl Acad Sci USA*,

739   http://dx.doi.org/10.1073/pnas.1423979112

740 Osborn, A.M., Moore, E.R., and Timmis, K.N. (2000) An evaluation of terminal-restriction

741   fragment length polymorphism (T-RFLP) analysis for the study of microbial community

742   structure and dynamics. *Environ Microbiol* **2:** 39–50.

743 Ottesen, E.A., Hong, J.W., Quake, S.R., and Leadbetter, J. R. (2006). Microfluidic digital

744   PCR enables multigene analysis of individual environmental bacteria. *Science* **314**: 1464–

745   1467.

746 Patil, K.R., Roune, L., and McHardy, A.C. (2012) The PhyloPythiaS web server for

747   taxonomic assignment of metagenome sequences. *PLoS ONE* **7**: e38581

748 Pester, M., and Brune, A. (2006) Expression profiles of fhs (FTHFS) genes support the

749   hypothesis that spirochaetes dominate reductive acetogenesis in the hindgut of lower

750   termites. *Environ Microbiol* **8:** 1261–1270.

751 Pester, M., and Brune, A. (2007) Hydrogen is the central free intermediate during

752   lignocellulose degradation by termite gut symbionts. *ISME J* **1:** 551–565.

753 Poehlein, A., Daniel, R., Schink, B., and Simeonova, D.D. (2013) Life based on phosphite: a

754   genome-guided analysis of *Desulfotignum phosphitoxidans*. *BMC Genomics* **14**: 753.

755 Prechtl, J., Kneip, C., Lockhart, P., Wenderoth, K., and Maier, U.-G. (2004) Intracellular

756   spheroid bodies of *Rhopalodia gibba* have nitrogen-fixing apparatus of cyanobacterial

757   origin. *Mol Biol Evol* **21**: 1477–81.

758 Rodionov, D.A., Dubchak, I., Arkin, A., Alm, E., and Gelfand, M.S. (2004) Reconstruction of

759 regulatory and metabolic pathways in metal-reducing δ-proteobacteria. *Genome Biol* **5**:

760 R90.

761 Reynolds, E.S. (1963) The use of lead citrate at high pH as an electron-opaque stain in

762 electron microscopy. *J Cell Biol* **17**: 208–212.

763 Rosenthal, A.Z., Zhang, X., Lucey, K.S., Ottesen, E.A., Trivedi, V., Choi, H.M.T., Pierce,

764 N.A., and Leadbetter, J.R. (2013) Localizing transcripts to single cells suggests an

765 important role of uncultured deltaproteobacteria in the termite gut hydrogen economy.

766 *Proc Natl Acad Sci USA* **110:** 16163–16168.

767 Sato, T., Hongoh, Y., Noda, S., Hattori, S., Ui, S., and Ohkuma, M. (2009) *Candidatus*

768 Desulfovibrio trichonymphae, a novel intracellular symbiont of the flagellate

769 *Trichonympha agilis* in termite gut. *Environ Microbiol* **11**: 1007–1015.

770 Schink, B., Thiemann, V., Laue, H., and Friedrich, M.W. (2002) *Desulfotignum*

771 *phosphitoxidans* sp. nov., a new marine sulfate reducer that oxidizes phosphite to

772 phosphate. *Arch Microbiol* **177**: 381–391.

773 Schuchmann, K., and Müller, V. (2012) A bacterial electron-bifurcating hydrogenase. *J Biol*

774 *Chem* **287:** 31165–3117.

775 Schuchmann, K., and Müller, V. (2014) Autotrophy at the thermodynamic limit of life: a

776 model for energy conservation in acetogenic bacteria. *Nat Rev Microbiol* **12:**809–821.

777 Schnell, S., Bak, F., and Pfennig, N. (1989) Anaerobic degradation of aniline and

778 dihydroxybenzenes by newly isolated sulfate-reducing bacteria and description of

779 *Desulfobacterium anilini. Arch Microbiol* **152;** 556–563.

780   Shinzato, N., Muramatsu, M., Matsui, T., and Watanabe,Y. (2007) Phylogenetic analysis of the

781   gut bacterial microflora of the fungus-growing termite *Odontotermes formosanus*. *Biosci*

782   *Biotechnol Biochem* **71:** 906–915.

783   Spurr, A.R. (1969) A low-viscosity epoxy resin embedding medium for electron microscopy. *J*

784   *Ultrastruct Res* **26**: 31–43.

785   Stingl, U., Radek, R., Yang, H., and Brune, A. (2005) '*Endomicrobia*': cytoplasmic symbionts

786   of termite gut protozoa form a separate phylum of prokaryotes. *Appl Environ Micobiol*

787   **71:** 1473–1479.

788   Suzuki, D., Li, Z., Cui, X., Zhang, C., and Katayama, A. (2014) Reclassification of

789   *Desulfobacterium anilini* as *Desulfatiglans anilini* comb. nov. within *Desulfatiglans* gen.

790   nov., and description of a 4-chlorophenol-degrading sulfate-reducing bacterium,

791   *Desulfatiglans parachlorophenolica* sp. nov. *Int J Syst Evol Microbiol* **64:** 3081–3086.

792   Strassert, J.F.H., Köhler, T., Wienemann, T.H.G., Ikeda-Ohtsubo, W., Faivre, N.,

793   Franckenberg, S., Plarre, R., Radek, R., and Brune, A. (2012) '*Candidatus* Ancillula

794   trichonymphae', a novel lineage of endosymbiotic *Actinobacteria* in termite gut

795   flagellates of the genus *Trichonympha*. *Environ Microbiol* **14**: 3259–3270.

796   Tai, V., and Keeling, P.J. (2013) Termite hindguts and the ecology of microbial communities

797   in the sequencing age. *J Euk Microbiol*, **60**: 421–428.

798   Trager, W. (1934) The cultivation of a cellulose-digesting flagellate, *Trichomonas*

799   *termopsidis*, and of certain other termite protozoa. *Biol Bull* **66**: 182–190.

800   Trinkerl, M., Breunig, A., Schauder, R. and König, H. (1990) *Desulfovibrio termitidis* sp.

801   nov., a carbohydrate-degrading sulfate-reducing bacterium form the hindgut of a termite.

802   *Syst Appl Microbiol* **13**: 372–377

803 Wang, S., Huang, H., Kahnt, J., and Thauer, R.K. (2013) A reversible electron-bifurcating

804   ferredoxin- and NAD dependent [FeFe]-hydrogenase (HydABC) in *Moorella*

805   *thermoacetica*. *J Bacteriol* **195:** 1267–1275.

806 Warnecke, F., Luginbühl, P., Ivanova, N., Ghassemian, M., Richardson, T.H., Stege, J.T., et al.

807   (2007) Metagenomic and functional analysis of hindgut microbiota of a wood feeding

808   higher termite. *Nature* **450**: 560–565.

809 Welte, C., and Deppenmeier, U. (2014) Bioenergetics and anaerobic respiratory chains of

810   aceticlastic methanogens. *Biochim Biophys Acta* **1837:** 1130–1147.

811 Widdel, F., and Bak, F. (1992) Gram-negative mesophilic sulfate-reducing bacteria. In *The*

812   *Prokaryotes, 2nd edn, Vol. 4* (Balows A., Trüper H.G., Dworkin M., Harder W., Schleifer

813   K.-H. (Eds). New York, NY, USA: Springer, pp. 3352–3378.

814 Yang, J., Xie, X., Wang, X., Dixon, R., and Wang, Y.P. (2014) Reconstruction and minimal

815   gene requirements for the alternative iron-only nitrogenase in *Escherichia coli*. *Proc Natl*

816   *Acad Sci USA* **111**: 3718–3725.

817 Zhang, X., Matson, E.G., and Leadbetter, J.R. (2011) Genes for selenium dependent and

818   independent formate dehydrogenase in the gut microbial communities of three lower,

819   wood-feeding termites and a wood-feeding roach. *Environ Microbiol* **13**: 307–323.

820 Zinoni, F., Birkmann, A., Leinfelder, W., and Böck, A. (1987) Cotranslational insertion of

821   selenocysteine into formate dehydrogenase from *Escherichia coli* directed by a UGA

822   codon. *Proc Natl Acad Sci USA* **84:** 3156–3160.

823 **Figure legends**

824 **Fig. 1.** Phylogenetic tree illustrating the position of '*Candidatus* Adiutrix intracellularis'

825 within the Rs-K70 group and relative to other *Deltaproteobacteria*. The maximum-likelihood

826 tree is based on an unambiguous alignment of 16S rRNA gene sequences (1,271 nucleotide

827 positions) and includes all phylotypes of the intestinal cluster obtained in this and previous

828 studies (for more details of the Rs-K70 group, see Fig. S1). Highly supported nodes (1,000

829 bootstraps) are marked (○, > 70%; ●, > 95%). The tree was rooted using representatives from

830 the other classes of *Proteobacteria* (not shown). Bar = 0.1 substitutions per site.

831

832 **Fig. 2.** Photomicrographs of *Trichonympha* flagellates and associated bacterial symbionts

833 from the hindgut of *Zootermopsis nevadensis*.

834 A. Epifluorescence image of a *Trichonympha* suspension simultaneously hybridized with a

835 fluorescein-labelled universal bacteria probe (EUB338, green) and a Cy3-labelled probe

836 specific for '*Ca.* Adiutrix intracellularis' (Delta-ZnvTr3; appears yellow in the overlay). Bar =

837 100 μm.

838 B. Phase-contrast image of a *Trichonympha collaris* cell, showing the nucleus and wood

839 particles in the posterior region. The arrow marks the outer cytoplasm of the anterior region,

840 which consists of cytoplasmic protrusions between the flagella. Bar = 50 μm.

841 C. Epifluorescence image of a *T. collaris* cell hybridized with probe Delta-ZnvTr3, showing

842 the distribution of '*Ca.* Adiutrix intracellularis' across the entire host cell. Bar = 50 μm.

843 D. The anterior pole of a *T. collaris* cell simultaneously hybridized with the same probe

844 (Delta-ZnvTr3; red) and a fluorescein-labelled probe (DSV698, green) matching the

845 *Desulfovibrio* symbiont; autofluorescent wood particles in vacuoles appear yellow. Bar = a,

846 100 μm; b–c, 50 μm; d, 10 μm.

847

848 **Fig. 3.** Transmission electron micrographs of *Trichonympha collaris* and its associated

849 symbionts.

850 A. Ultrathin section of the posterior part of the host cell, showing endosymbiotic '*Ca.*

851 Adiutrix intracellularis' (arrows) surrounded by hydrogenosomes (h); the inset shows a

852 longitudinal section of the endosymbiont. Bar = 1 μm (inset: 0.2 μm).

853 B. Radial section of the cytoplasmic lamellae between the flagella (fl) in the collar region,

854 showing endosymbiotic '*Ca.* Adiutrix intracellularis' (black arrows) and ectosymbiotic '*Ca.*

855 Desulfovibrio trichonymphae' (white arrows). Bar = 1 μm.

856 C. Longitudinal section of the same region, showing '*Ca.* Adiutrix intracellularis' (black

857 arrows) and '*Ca.* Desulfovibrio trichonymphae' (white arrows) and multiple rows of flagella

858 (fl). Bar = 1 μm.

859

860 **Fig. 4.** Wood-Ljungdahl pathway for reductive acetogenesis and energy conservation in '*Ca.*

861 Adiutrix intracellularis'. The scheme is based on the annotation of the draft genome of strain

862 Adiu1 (Table S4). Colors indicate the phylogenetic context of the respective homologs in

863 published genomes: blue, *Deltaproteobacteria* (sulfate reducers); red, *Clostridiales*

864 (homoacetogens); green, *Treponema primitia* (homoacetogen). A detailed analysis of each

865 gene homolog potentially involved in the Wood-Ljungdahl pathway and the energy

866 metabolism in this context is shown in Table S5. The hypothetical link (dotted lines) between

867 the energy-converting 11-subunit complex and methylene-THF reductase is discussed in the

868 text.

869

870 **Fig. 5.** Metabolic map of '*Ca.* Aduitrix intracellularis' reconstructed from the draft genome of

871 strain Adiu1. Important cofactors in energy metabolism (in red) and the links to the pathways

872 of amino acid biosynthesis (in blue) and vitamin and cofactor biosynthesis (in orange) are

873 emphasized. Abbreviations: THF, tetrahydrofolate; HCO-THF, 10-formyl-tetrahydrofolate;

874 CH_2=THF, 5,10-methylenetetrahydrofolate; CH_3-THF, 5-methyltetrahydrofolate, CFeSP,

875 corrinoid iron–sulfur protein; Acetyl-P; acetyl phosphate; G1P, glucose 1-phosphate; G6P,

876 glucose 6-phosphate; M6P, mannose 6-phosphate; F6P, fructose 6-phosphate; FBP, fructose

877 1,6-bisphosphate; GAP, glyceraldehyde 3-phosphate; BPG, 1,3-bisphosphoglycerate; 3PG, 3-

878 phosphoglycerate, 2PG, 2-phosphoglycerate; PEP, phosphoenolpyruvate; E4P, erythrose 4-

879 phosphate; S7P, sedoheptulose 7-phosphate; X5P, xylulose 5-phosphate; R5P, ribose-5-

880 phosphate; Ru5P, ribulose 5-phosphate; PRPP, phosphoribosyl pyrophosphate; Ala, alanine;

881 Arg, arginine; Asp, aspartate; Asn, asparagine; Glu, glutamate; Gln, glutamine; Gly, glycine;

882 Ile, isoleucine; Leu, leucine; Lys, lysine; Phe, phenylalanine; Pro, proline; Ser, serine; Thr,

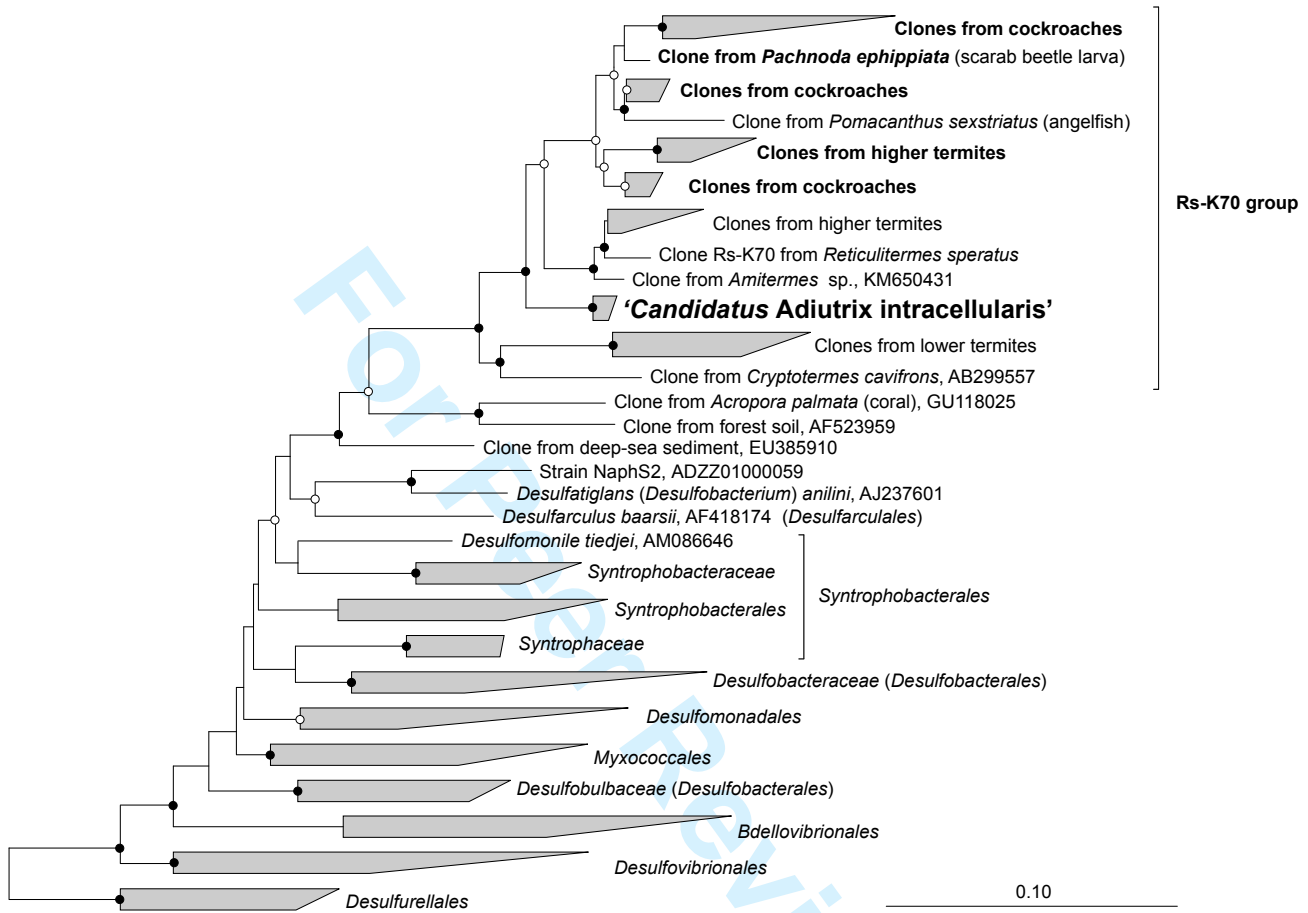883 threonine; Trp, tryptophan; Tyr, tyrosine; Val, valine.
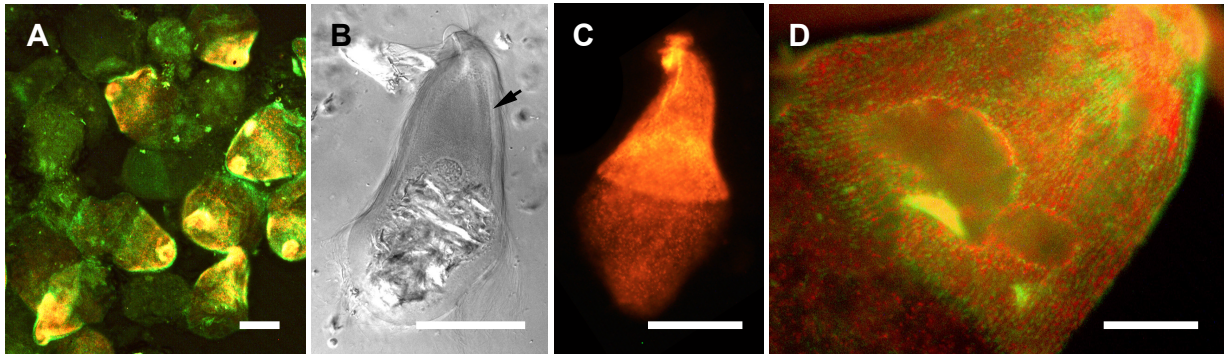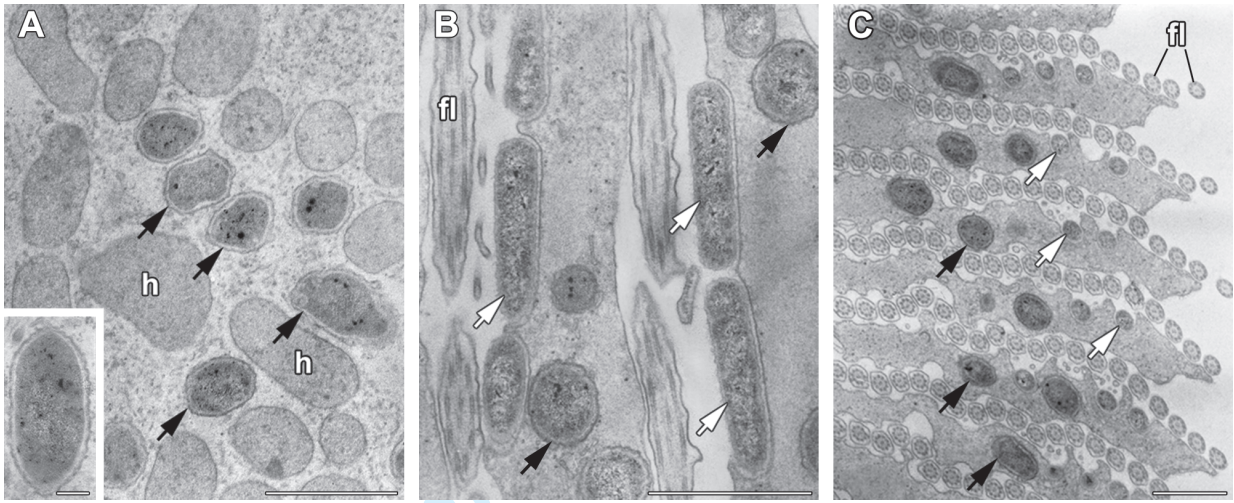
Fig. 1

Fig. 2

Fig. 3

Fig. 4

H₂ ... 2 H₂ ... n Na⁺/H⁺ ... CO₂

hydA2 *hydABC*
hycB2 *hndABC*
hycB3

nuoABCD
HIJKLMN

NAD⁺ Fd$_{ox}$ Fd$_{red}$ Fd$_{ox}$
NADH Fd$_{red}$ Fd$_{ox}$ A$_{red}$ Fd$_{red}$

A$_{ox}$

hdrABC   *acsA*
mvhD   *BCD*

CO₂ → HCOOH → CHO-THF → CH₂=THF → CH₃-THF → CoA
      ATP   NAD(P)H

fdhF$_{Cys}$ *ftcD* *folD*   *metVF*
fdhF$_{Sec}$ *fhs* *fchA*

THF ← AcCoA → Ac-P → Acetate
                pta   ATP *ackA*

Fig. 5